

# Interpreting virtual photon interactions in terms of parton distribution functions <sup>1</sup>

J. Chýla<sup>a</sup>, M. Taševský<sup>a</sup>

<sup>a</sup> Institute of Physics, Prague, Na Slovance 8, Prague 8, Czech Republic

**Abstract:** Interactions of virtual photons are analyzed in terms of photon structure. It is argued that the concept of parton distribution functions is phenomenologically very useful even for highly virtual photons involved in hard collisions. The role of longitudinal photons for proper interpretation of jet cross-sections in the region of moderate virtualities accessible at HERA is investigated.

## 1 Introduction

In quantum field theory it is difficult to distinguish effects of the “structure” from those of “interactions”. Within the Standard Model it makes good sense to distinguish *fundamental particles*, which correspond to fields in its lagrangian  $\mathcal{L}_{\text{SM}}$  (leptons, quarks, gauge and Higgs bosons) from *composite particles*, like atoms or hadrons, which appear in the mass spectrum but have no corresponding field in  $\mathcal{L}_{\text{SM}}$ . For the latter the use of parton distribution functions (PDF) to describe their “structure” appears natural, but the concept of PDF turns out to be phenomenologically useful also for some fundamental particles, in particular the photon. PDF are indispensable for the real photon due to strong interactions between the pair of quarks to which it couples electromagnetically. For massless quarks this coupling leads to parallel singularities, which must be absorbed in PDF of the photon. For nonzero photon virtualities there is no true singularity associated with the coupling  $\gamma \rightarrow q\bar{q}$  and therefore no real need for PDF. The main aim of this paper is to advocate the use of PDF even for the virtual photon.

## 2 PDF of the real photon

The factorization scale dependence of PDF of the real photon is determined by the system of coupled inhomogeneous evolution equations

$$\frac{d\Sigma(M^2)}{d \ln M^2} = k_q + P_{qq} \otimes \Sigma + P_{qG} \otimes G, \quad (1)$$

$$\frac{dG(M^2)}{d \ln M^2} = k_G + P_{Gq} \otimes \Sigma + P_{GG} \otimes G, \quad (2)$$

$$\frac{dq_{\text{NS}}(M^2)}{d \ln M^2} = \sigma_{\text{NS}} k_q + P_{\text{NS}} \otimes q_{\text{NS}}, \quad (3)$$

---

<sup>1</sup>Contribution to the Workshop *Monte Carlo generators for HERA Physics*, DESY, 1998–1999

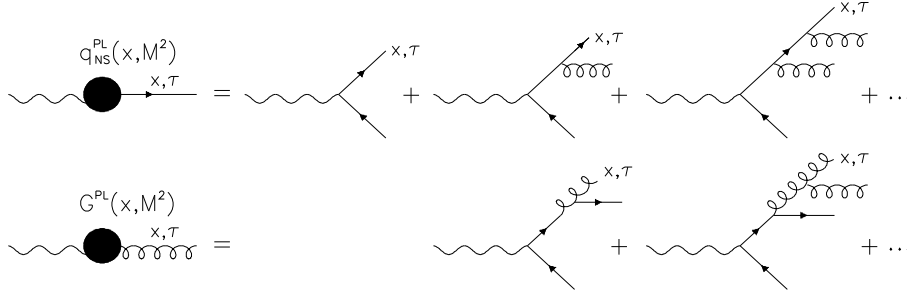


Figure 1: *Diagrams defining the pointlike parts of quark and gluon distribution functions in LL approximation. The resummation involves integration over parton virtualities  $M_0^2 \leq \tau \leq M^2$ .*

for singlet, nonsinglet and gluon distribution functions. The splitting functions  $k_q, k_G$  and  $P_{ij}$  admit expansions in powers of  $\alpha_s$ ,

$$k_q(x, M) = \frac{\alpha}{2\pi} \left[ k_q^{(0)}(x) + \frac{\alpha_s(M)}{2\pi} k_q^{(1)}(x) + \left( \frac{\alpha_s(M)}{\pi} \right)^2 k_q^{(2)}(x) + \dots \right], \quad (4)$$

$$k_G(x, M) = \frac{\alpha}{2\pi} \left[ \frac{\alpha_s(M)}{2\pi} k_G^{(1)}(x) + \left( \frac{\alpha_s(M)}{\pi} \right)^2 k_G^{(2)}(x) + \dots \right], \quad (5)$$

$$P_{ij}(x, M) = \frac{\alpha_s(M)}{2\pi} P_{ij}^{(0)}(x) + \left( \frac{\alpha_s(M)}{2\pi} \right)^2 P_{ij}^{(1)}(x) + \dots, \quad (6)$$

which start at the order  $\alpha\alpha_s$ , except for  $k_q$  for which  $k_q^{(0)} = 3e_q^2(x^2 + (1-x)^2) = O(1)$ . The general solution of these equations can be written as the sum of a particular solution of the full inhomogeneous equations and the general solution of the corresponding homogeneous ones, called *hadronic* (or VDM) part. A subset of solutions of the inhomogeneous evolution equations resulting from the resummation of diagrams in Fig. 1 defines the so called *pointlike* (PL) parts. This resummation softens the  $x$ -dependence of  $q^{\text{PL}}(x, M^2)$  with respect to the term  $(\alpha/2\pi)k_{\text{NS}}^{(0)}(x)$ , corresponding to the simple  $\gamma \rightarrow q\bar{q}$  splitting. A general solution of eqs. (1-2) can thus be written as ( $D = q, \bar{q}, G$ )

$$D(x, M^2) = D^{\text{PL}}(x, M^2) + D^{\text{VDM}}(x, M^2), \quad D = q, \bar{q}, G. \quad (7)$$

The important point to keep in mind is the fact that there is an infinite number of pointlike solutions  $q^{\text{PL}}(x, M^2), G^{\text{PL}}(x, M^2)$ , differing merely by the initial scale  $M_0$  at which they vanish. Consequently, the separation of quark and gluon distribution functions into their pointlike and VDM parts is ambiguous and these concepts have thus separately no physical meaning <sup>2</sup>.

## 2.1 Properties of Schuler–Sjöstrand parametrizations

Practical aspects of the ambiguity in separating PDF into their VDM and pointlike parts can be illustrated on the properties of SaS1D and SaS2D parametrizations [1, 2], which differ by the choice of initial  $M_0$ :  $M_0 = 0.6$  GeV for SaS1D,  $M_0 = 2$  GeV for SaS2D. What makes the SaS approach particularly useful for our discussion is the fact that it provides separate parametrizations of the VDM and pointlike parts of both quark and gluon distributions. In

<sup>2</sup>For brevity the terms “pointlike quarks” and “pointlike gluons” will hence be employed to denote pointlike parts of quark and gluon distribution functions of the photon.

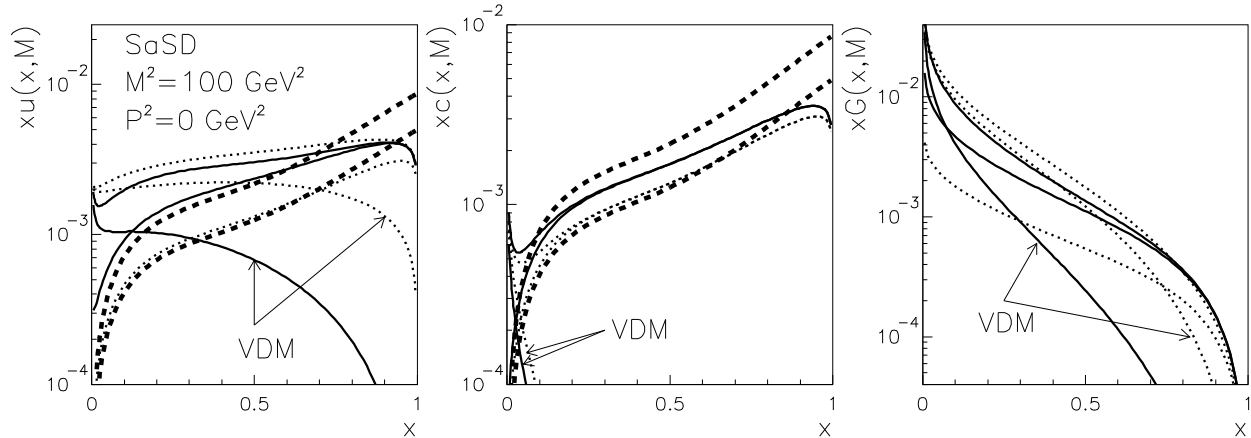


Figure 2: *The  $u$  and  $c$  quark and gluon distribution functions of the real photon for SaS1D (upper solid curves) and SaS2D (upper dotted curves) parametrizations at  $M^2 = 100 \text{ GeV}^2$ . The VDM and pointlike (solid and dotted curves peaking at large  $x$ ) parts of both parametrizations are plotted separately. For quarks the splitting terms corresponding to SaS1D (upper dashed curves) and SaS2D (lower dashed curves) parametrizations are overlaid.*

Fig. 2 we compare distribution functions  $xu(x, M^2)$ ,  $xc(x, M^2)$  and  $xG(x, M^2)$  as given by SaS1D and SaS2D parametrizations at  $M^2 = 100 \text{ GeV}^2$ . To see the effects of the resummation of multiple parton emission we also plot the corresponding splitting terms

$$q^{\text{split}}(x, M_0^2, M^2) \equiv \frac{\alpha}{2\pi} 3e_q^2 (x^2 + (1-x)^2) \ln \frac{M^2}{M_0^2}. \quad (8)$$

In Fig. 3 we illustrate in two ways the scale dependence of VDM and pointlike parts of the same three distribution functions. In the upper six plots we compare them as a function of  $x$  at  $M^2 = 25, 100, 1000 \text{ GeV}^2$ , while in the lower three plots the same distributions are rescaled by the factor  $\ln(M^2/M_0^2)$ . Finally, in Figs. 4 and 5 we compare LO SaS predictions for two physical quantities:  $F_2^\gamma$  and effective parton distribution function  $D_{\text{eff}}$ , relevant for approximate calculations of jet production

$$F_2^\gamma(x, Q^2) = \sum_{i=1}^{n_f} 2xe_i^2 q_i(x, Q^2), \quad (9)$$

$$D_{\text{eff}}(x, M^2) = \sum_{i=1}^{n_f} (q_i(x, M^2) + \bar{q}_i(x, M^2)) + \frac{9}{4}G(x, M^2). \quad (10)$$

Figures 2–5 illustrate several important properties of PDF of the real photon:

- There is a huge difference between the relative importance of VDM components in SaS1D and SaS2D parametrizations: for SaS2D the VDM components of  $xu(x, M)$  and  $xG(x, M)$  are dominant up to  $x \doteq 0.75$ , whereas for SaS1D the pointlike one dominates already above  $x \doteq 0.1$ !
- Factorization scale dependence of VDM and pointlike parts differ substantially. VDM components exhibit the pattern of scaling violations typical for hadrons, whereas the pointlike parts of both quark and gluon distribution functions rise with  $M$  for all  $x$ . For

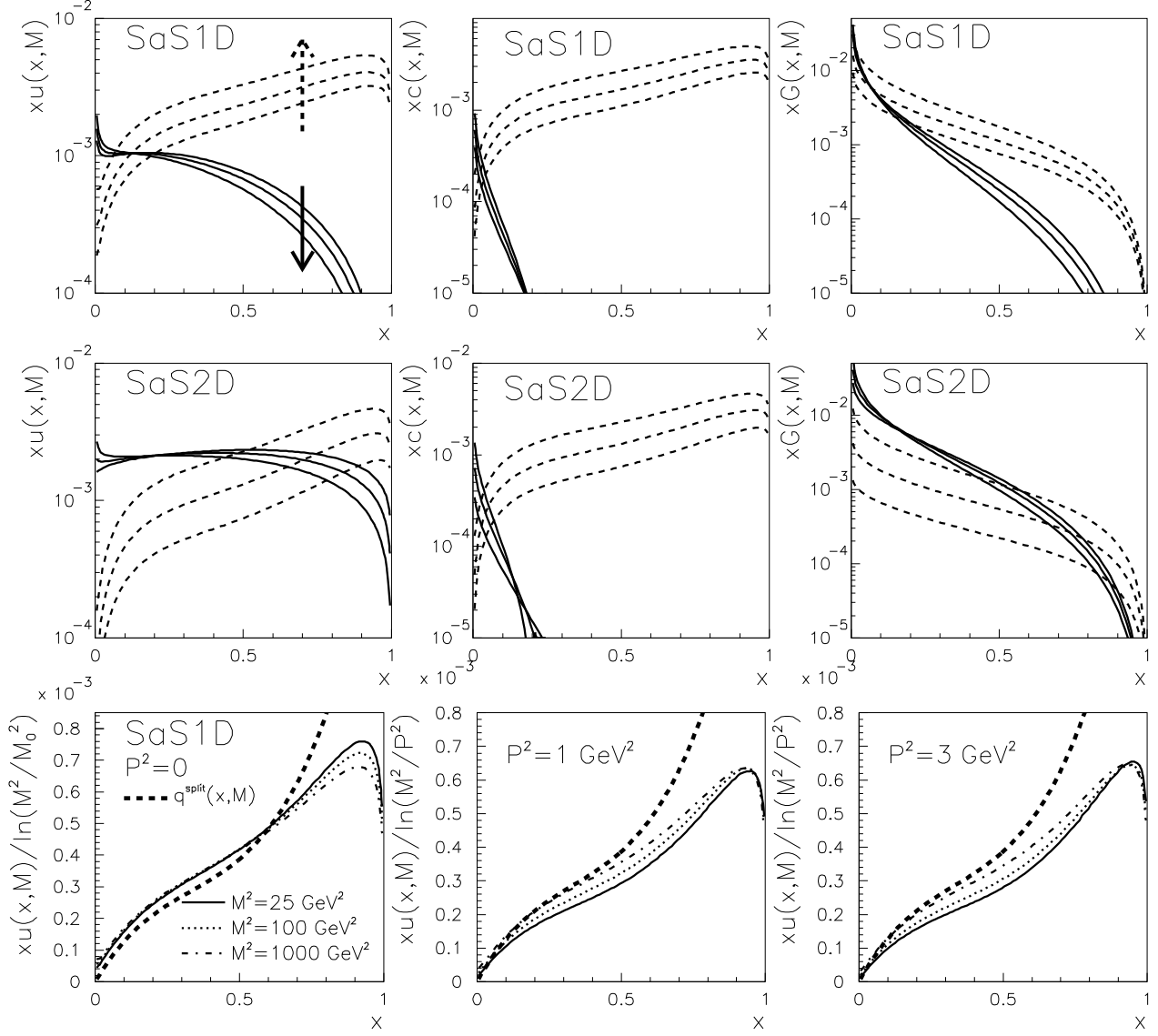


Figure 3: Factorization scale dependence of parton distributions functions  $u(x, M)$ ,  $c(x, M)$  and  $G(x, M)$  of the real photon. Dashed curves correspond, in the order indicated by the arrows, to pointlike and solid to VDM parts of these distributions at  $M^2 = 25, 100$  and  $1000 \text{ GeV}^2$ . The meaning of arrows is the same for all parton distribution functions. In the lower part SaS1D quark distribution functions  $xu(x, M^2, P^2)$  scaled by  $\ln(M^2/M_0^2)$  for the real photon (left) and by  $\ln(M^2/P^2)$  for the virtual one, are plotted and compared to the predictions of the splitting term (8).

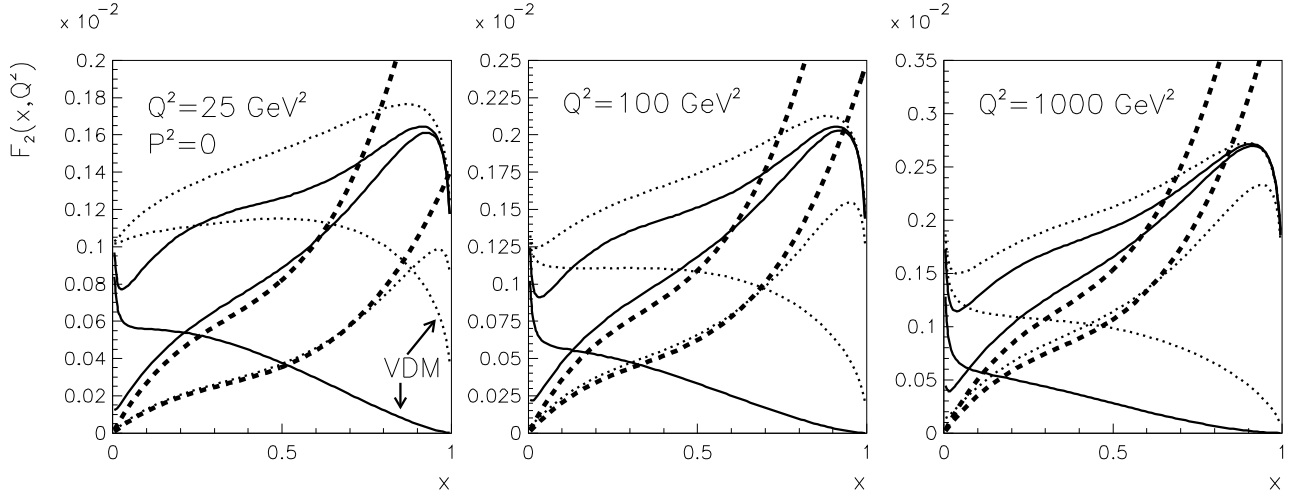


Figure 4:  $F_2^\gamma(x, Q^2)$  as a function of  $x$  for  $Q^2 = 25, 100, 1000 \text{ GeV}^2$  as given by SaS1D (solid curves) and SaSD2 (dotted curves) parametrizations. The full results are given by the upper, the VDM and pointlike contributions parts by two lower curves. The dashed curves describe the contributions of the splitting term (8) with  $M_0 = 0.6 \text{ GeV}$  for SaS1D and  $M_0 = 2 \text{ GeV}$  for SaSD2.

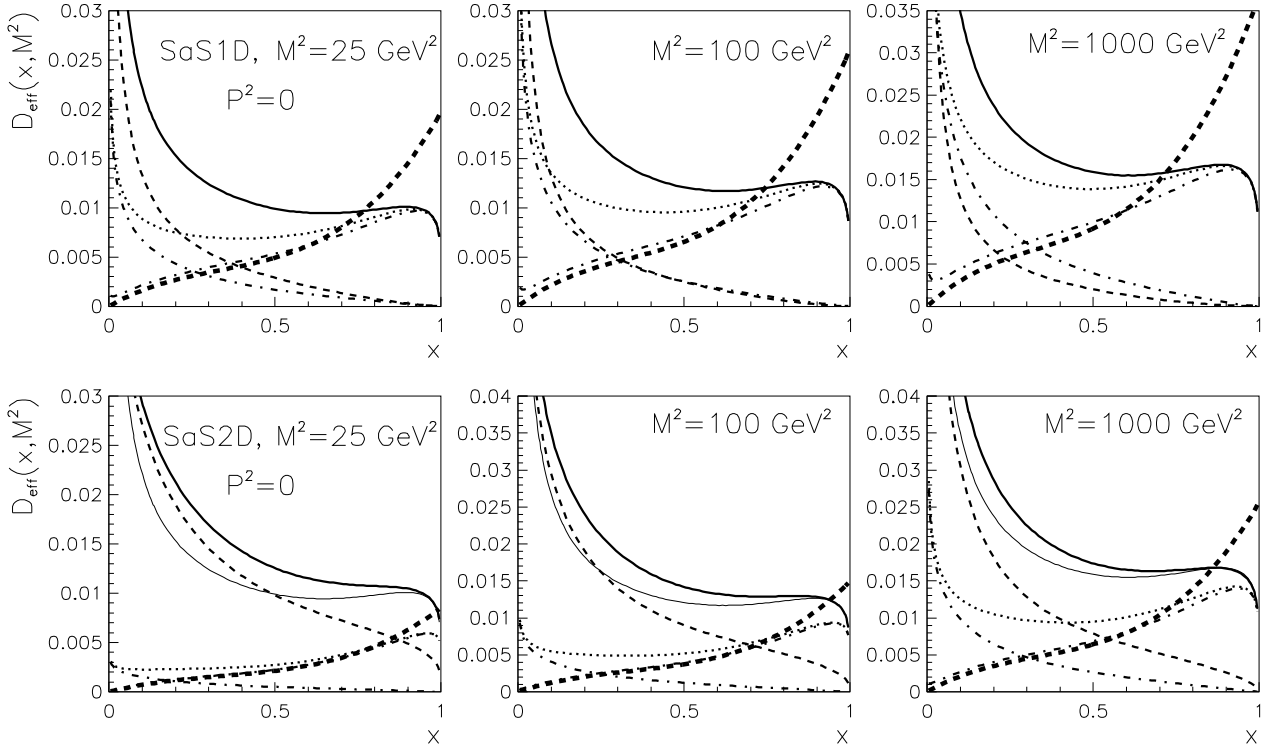


Figure 5:  $D_{\text{eff}}(x, M^2)$  as a function of  $x$  for  $M^2 = 25, 100, 1000 \text{ GeV}^2$  for the real photon as given by SaS1D and SaSD2 parametrizations. Solid curves show the full results, dashed ones the VDM and dotted ones the pointlike parts. The pointlike part is further separated into the contributions of pointlike quarks and pointlike gluons, denoted by two dash-dotted curves (those peaking at low  $x$  correspond to gluons). Thick dashed curves correspond to the splitting term (8). The thin solid curves in SaSD2 plots show the full results of the SaS1D parametrization.

pointlike gluons this holds despite the fact that  $G^{\text{PL}}(x, M^2)$  satisfies at the LO standard homogeneous evolution equation and is due to the fact that its evolution is driven by the rise of  $\Sigma^{\text{PL}}(x, M^2)$ .

- As the factorization scale  $M$  increases the VDM parts of both quark and gluon distribution functions decrease relative to the pointlike ones, except in the region of very small  $x$ .
- Despite huge differences between SaS1D and SaS2D parametrizations in the decomposition of quark and gluon distributions into their VDM and pointlike parts, their predictions for physical quantities  $F_2^\gamma$  and  $D_{\text{eff}}$  are quite close.
- The most prominent effect of multiple parton emission on physical quantities appears to be the contribution of pointlike gluons to jet cross-sections in the region  $x_\gamma \lesssim 0.5$ .

### 3 PDF of the virtual photon: do we really need them?

For sufficiently virtual photon the initial state singularity resulting from the splitting  $\gamma^* \rightarrow q\bar{q}$  is shielded off by the nonzero initial photon virtuality  $P^2$  and therefore in principle the concept of PDF does not have to be introduced. Nevertheless, even in such circumstances PDF turn out to be phenomenologically very useful because their pointlike parts include the resummation of parts of higher order QCD corrections, and the VDM parts, though decreasing rapidly with increasing  $P^2$ , are still dominant at very small  $x_\gamma$ . Both of these aspects define the “nontrivial” structure of the virtual photon in the sense that they are not included in the splitting term (8) and thus are not part of existing NLO unsubtracted direct photon calculations.

#### 3.1 Virtuality dependent PDF

In QCD the nonperturbative effects connected with the confinement are expected to determine the long-range structure of the photon and hence also the transition between the virtual and real photon. As for the real photon, we recall basic features of SaS parametrizations of PDF of the virtual photon. We refer the reader to the web version of this contribution for the figures illustrating the following observations.

- Both VDM and pointlike parts drop with increasing  $P^2$ , but VDM parts drop much faster.
- With increasing  $P^2$  the relative importance of VDM parts of both quark and gluon distribution functions decreases rapidly. For  $M^2 \geq 25 \text{ GeV}^2$  the VDM parts of both SaS1D and SaS2D parametrizations become practically negligible already at  $P^2 \approx 3 \text{ GeV}^2$ , except in the region of very small  $x \lesssim 0.01$ . Hence, also the ambiguity in the separation (7) is largely irrelevant in this region.
- The general pattern of scaling violations remains the same as for the real photon, except for a subtle difference, best visible (see Fig. 3) when comparing the rescaled PDF for  $P^2 = 0$  with those at  $P^2 = 1, 3 \text{ GeV}^2$ . While for  $P^2 = 0$  the SaSD1 parametrizations of quark distribution functions soften with increasing  $M^2$  and intersect the splitting term at  $x \simeq 0.65$ , for  $P^2 \geq 1 \text{ GeV}^2$  they rise with  $M^2$  for all  $x$  and stay above the splitting term. These properties reflect the fact that SaS parametrizations of PDF of the virtual photon do not satisfy the same evolution equations as PDF of the real one.

- Pointlike quarks dominate  $D_{\text{eff}}(x, P^2, M^2)$  at large  $x$ , while for  $x \lesssim 0.5$ , most of the pointlike contribution comes from the pointlike gluons. In particular, the excess of the pointlike contributions to  $D_{\text{eff}}$  over the contribution of the splitting term, observed at  $x \lesssim 0.5$ , comes almost entirely from the pointlike gluons!
- For  $x \gtrsim 0.6$  the full results are below those given by the splitting term (8) with  $M_0^2 = P^2$  and one therefore expects the sum of subtracted direct and resolved contributions to jet cross-sections to be smaller than the results of unsubtracted direct calculations.

Jet production in ep collisions at HERA in the region of photon virtualities  $P^2 \gtrsim 1$  thus offers a promising opportunity for the identification of nontrivial aspects of PDF of virtual photons at both small (but not very small) and large values of  $x$ . All these conclusions were obtained within the simple LO formalism, but as shown in the next Section they hold within the framework of NLO parton level calculations as well.

### 3.2 Should we care about $\gamma_L^*$ ?

Most of the existing phenomenological analyses of the properties and interactions of virtual photons as well as all available parametrizations of their PDF concern transverse photons only. Neglecting longitudinal photons is a good approximation for  $y \rightarrow 1$ , where the flux  $f_L^\gamma(y, P^2) \rightarrow 0$ , as well as for very small virtualities  $P^2$ , where PDF of  $\gamma_L^*$  vanish by gauge invariance. But how small is “very small” in fact? For instance, should we take into account the contribution of  $\gamma_L^*$  to jet cross-section in the region  $E_T^{\text{jet}} \gtrsim 5 \text{ GeV}$ ,  $P^2 \gtrsim 1 \text{ GeV}^2$ , where most of the data on virtual photons extracted from ep collisions at HERA come from? Despite the fact that the structure of longitudinal photons has not yet been investigated experimentally and is also poorly known theoretically, simple parton model estimates (see [3] for details) of their effects suggest that in the mentioned kinematical region  $\gamma_L^*$  must be taken into account in the resolved photon contribution but may be safely neglected in the direct one. This difference comes from the fact that at small  $P^2$  the contributions of  $\gamma_L^* L$  to physical cross-sections behave as  $P^2/\hat{s}$  (i.e. vanish for fixed  $P^2$  when  $\hat{s} \rightarrow \infty$ ) in the direct channel, but as  $P^2/\mu^2$  (with  $\mu$  a fixed parameter) in the resolved part. In simple QED based considerations  $\mu$  is given by quark masses, while in realistic QCD we expect it to be given by some nonperturbative parameter of the order of 1 GeV. To assess the importance of  $\gamma_L^*$ , LO expressions for  $D_{\text{eff}}(x, P^2, M^2)$  evaluated with SaS1D parametrizations for  $\gamma_T^*$ , are compared in Fig. 6 with the formula (44) of [3] for the quark distribution function of  $\gamma_L^*$ , treating  $m$  in the latter as a free parameter. The dotted curves in this figure correspond (from below) to  $m^2 = 1 \text{ GeV}^2$ ,  $m^2 = 0.1 \text{ GeV}^2$  and to the asymptotic expression  $(\alpha/2\pi)12e_q^2x(1-x)$ , obtained in the limit  $m \rightarrow 0$ . As expected, the importance of  $\gamma_L^*$  depends sensitively on  $m$ . Moreover, its contributions relative to those of  $\gamma_T^*$  peak at about  $x \approx 0.65$ , drop with increasing  $M^2$  (for  $P^2$  and  $m^2$  fixed), and with increasing  $m^2$  (for  $P^2$  and  $M^2$  fixed). Fig. 6 suggests that in the kinematical region accessible at HERA the contributions of  $\gamma_L^*$  should be taken into account in phenomenological analyses of data on virtual photon interactions. Better theoretical knowledge of the structure of  $\gamma_L^*$  is clearly needed.

In all considerations of this subsection we simply added the contributions of  $\gamma_T^*$  and  $\gamma_L^*$ , despite the fact that the respective fluxes  $f_T^\gamma(y, P^2)$ ,  $f_L^\gamma(y, P^2)$  differ. Our conclusions are

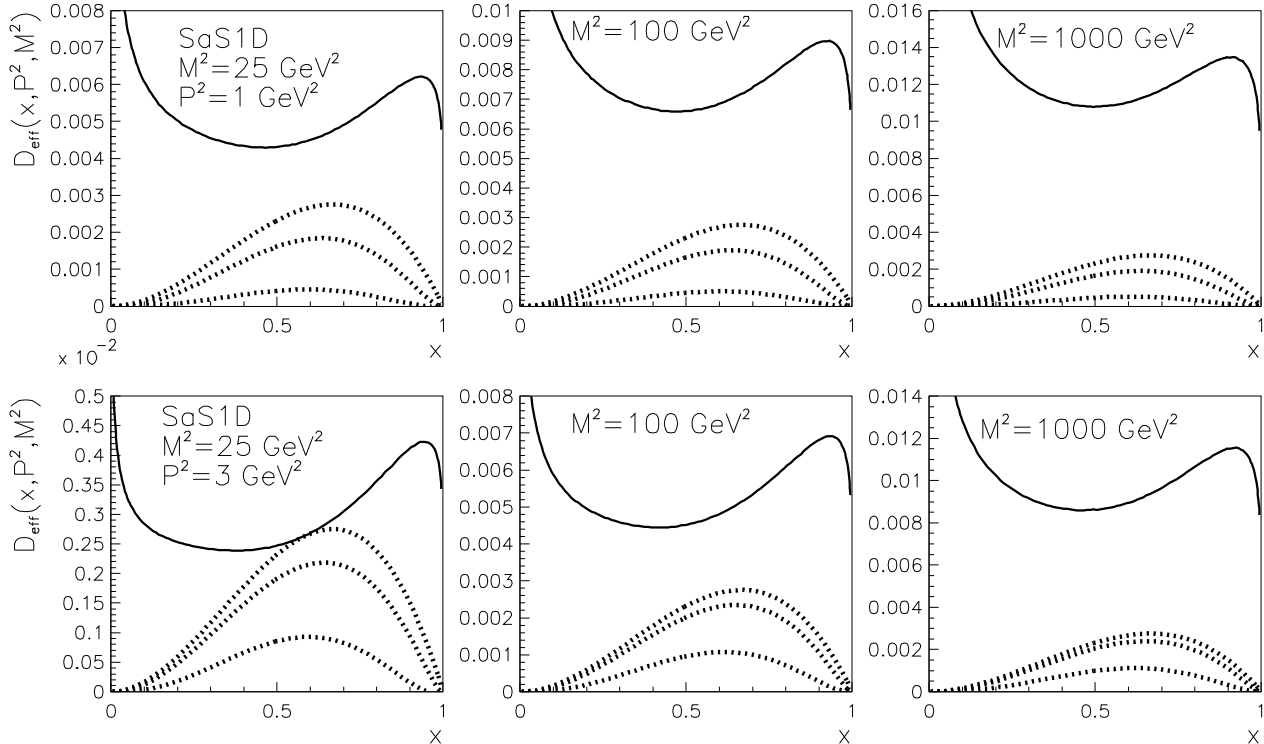


Figure 6:  $D_{\text{eff}}(x, P^2, M^2)$  calculated from *SaS1D* parametrizations for  $\gamma_T^*$  (solid curves) compared to results for  $\gamma_L^*$  displayed by dotted curves and corresponding from above to  $m^2 = 0, 0.1$  and  $1 \text{ GeV}^2$ .

therefore directly relevant for small values of  $y$  only<sup>3</sup>, but it is trivial to modify the above considerations by taking the respective fluxes properly into account.

## 4 PDF of the virtual photon in NLO QCD calculations

In [4] data on dijet production in the region of photon virtualities  $1 \leq P^2 \leq 50 \text{ GeV}^2$ , and for jet transverse energies  $E_T^{\text{jct}} \geq 5 \text{ GeV}$  have been analyzed within the framework of effective PDF defined in (10). This analysis shows that in the kinematical range  $1 \text{ GeV}^2 \lesssim P^2 \lesssim E_T^2$  the data agree reasonably with the expectations based on SaS parametrizations of PDF of the virtual photon. The same data may, however, be also analyzed using the NLO parton level Monte-Carlo programs that do not introduce the concept of PDF of virtual photons, like DISENT, MEPJET or DISASTER++. Nevertheless, so long as  $P^2 \ll M^2 \approx E_T^2$ , the pointlike parts of PDF incorporate numerically important effects of a part of higher order corrections, namely those coming from collinear emission of partons in Fig. 1. To illustrate this point we shall now discuss dijet cross-sections calculated by means of JETVIP [5], currently the only NLO parton level Monte-Carlo program that includes both the direct and resolved photon contributions.

All the above mentioned parton level NLO MC programs contain the same full set of partonic cross-sections<sup>4</sup> for the direct photon contribution up the order  $\alpha\alpha_s^2$ . In addition JETVIP

<sup>3</sup>Note, however, that even at  $y = 0.4$  the ratio  $f_T^\gamma(y, P^2)/f_L^\gamma(y, P^2) = 1.16$  is still quite close to 1.

<sup>4</sup>In this subsection the various terms considered are characterized by the powers of  $\alpha$  and  $\alpha_s$  appearing in hard scattering cross-sections. Writing  $O(\alpha^j \alpha_s^k)$  will thus mean terms proportional to  $\alpha^j \alpha_s^k$ , not terms up



includes also the resolved photon contribution. Once the concept of virtual photon structure is introduced, part of the direct photon contribution, namely the splitting term (8), is subtracted from it and included in PDF appearing in the resolved photon contribution. To avoid confusion we shall use the term “direct unsubtracted” ( $\text{DIR}_{\text{uns}}$ ) to denote complete NLO direct photon contribution and reserve the term “direct” (DIR) for the results after this subtraction. In this terminology the complete NLO calculations is given by the sum of direct and resolved parts and denoted DIR+RES.

For complete  $O(\alpha_s^2)$  calculations only the LO resolved photon contribution must be added to the  $O(\alpha\alpha_s^2)$  direct one. However, for reasons outlined in the next subsection, JETVIP includes also NLO resolved contributions. This might seem inconsistent as the corresponding  $O(\alpha\alpha_s^3)$  direct photon terms are not yet available and thus not included. Nevertheless, this procedure makes sense precisely because of a clear physical meaning of PDF of the virtual photon!

## 4.1 Factorization mechanism in $\gamma p$ interactions

The main argument for adding  $O(\alpha_s^3)$  resolved photon terms to  $O(\alpha\alpha_s^2)$  direct and  $O(\alpha_s^2)$  resolved photon contributions is based on specific way factorization mechanism works for processes involving initial photons. This point is crucial but subtler and we therefore merely summarize the conclusions and refer the reader to the website version of this contribution, or to [3], for details. In the absence of  $O(\alpha\alpha_s^3)$  direct calculations, we have two options:

- To stay within the framework of complete  $O(\alpha_s^2)$  calculations, including the LO resolved and NLO direct contributions, but with no mechanism for the cancellation of the dependence of PDF of the virtual photon on the factorization scale  $M$ .
- To add to the previous framework the  $O(\alpha_s^3)$  resolved photon contributions, which provide necessary cancellation mechanism with respect to the part of factorization scale dependence of photonic PDF “generated” by the homogeneous part of the evolution equations (1–3). The drawback of this procedure is the fact that the NLO resolved photon terms do not represent a complete set of  $O(\alpha_s^3)$  contributions.

In our view the second strategy, adopted in JETVIP, is more appropriate. In fact one can look at  $O(\alpha_s^3)$  resolved photon terms as results of approximate evaluation of the so far uncalculated  $O(\alpha\alpha_s^3)$  direct photon diagrams in the collinear kinematics. There are of course  $O(\alpha\alpha_s^3)$  direct photon contributions that cannot be obtained in this way, but we are convinced that it makes sense to build phenomenology on this framework.

Note that for the  $O(\alpha_s^2)$  resolved terms the so far unknown  $O(\alpha\alpha_s^3)$  direct photon contributions provide the first chance to generate pointlike gluons inside the photon. To get the gluon in  $O(\alpha_s^3)$  resolved photon contributions would require evaluating diagrams of even higher order  $O(\alpha\alpha_s^4)$ ! In summary, although the pointlike parts of quark and gluon distribution functions of the virtual photon are in principle included in higher order perturbative corrections and can therefore be considered as expressions of “interactions” rather than “structure”, their uniqueness and phenomenological usefulness definitely warrant their introduction as well as their names.

---

*to* this order! For approximations taking into account the first two or three powers of  $\alpha_s$ , in either direct or resolved channel, the denomination NLO and NNLO are used.

## 4.2 Dijet production at HERA

To make our conclusions potentially relevant for analyses of HERA data on jet production we have chosen the following kinematical region (jets with highest and second highest  $E_T$  are labelled “1” and “2”)

**Jet transverse energies:** asymmetric cuts  $E_T^{(1)} \geq 7 \text{ GeV}$ ,  $E_T^{(2)} \geq 5 \text{ GeV}$ ;

**Photon virtuality:** four windows in  $P^2$

$$1.4 \leq P^2 \leq 2.4 \text{ GeV}^2; \quad 2.4 \leq P^2 \leq 4.4 \text{ GeV}^2; \quad 4.4 \leq P^2 \leq 10 \text{ GeV}^2; \quad 10 \leq P^2 \leq 25 \text{ GeV}^2$$

**Jet pseudorapidities** in  $\gamma^*$  CMS:  $-2.5 \leq \eta^{(i)} \leq 0$ ,  $i = 1, 2$

The cuts were chosen in such a way that throughout the region  $P^2 \ll E_T^2$ , thereby ensuring that the virtual photon lives long enough for its “structure” to develop before the hard scattering takes place. As far as jet transverse energies are concerned, we have chosen the asymmetric cut scenario:  $E_T^{(1)} \geq E_T^c + \Delta$ ,  $E_T^{(2)} \geq E_T^c$ , which avoids the problems [6] coming from the region where  $E_T^{(1)} \approx E_T^{(2)}$ . The asymmetric cut option is appropriate if one plots separately the  $E_T^{(1)}$  and  $E_T^{(2)}$  distributions, or, as we do, their sum, called distribution of “trigger jets” [5]. To determine the value of  $\Delta$  optimally, we evaluated the integral  $\sigma(\Delta)$  over the selected region in  $E_T^{(1)} - E_T^{(2)}$  plane as a function of  $\Delta$  and on the basis thereof took  $\Delta = 2 \text{ GeV}$  for all  $P^2$ .

In our analysis jets are defined by means of the cone algorithm. At NLO parton level all jet algorithms are essentially equivalent to the cone one, supplemented with the parameter  $R_{\text{sep}}$ , introduced in order to bridge the gap between the application of the cone algorithm to NLO parton level calculations and to hadronic systems (from data or MC), where one encounters ambiguities concerning the seed selection and jet merging. In a general cone algorithm two objects (partons, hadrons or calorimetric cells) belong to a jet if they are within the distance  $R$  from the jet center. Their relative distance satisfies, however, a weaker condition

$$\Delta R_{ij} = \sqrt{(\Delta\eta_{ij})^2 + (\Delta\phi_{ij})^2} \leq \frac{E_{T_i} + E_{T_j}}{\max(E_{T_i}, E_{T_j})} R. \quad (11)$$

The parameter  $R_{\text{sep}}$  governs the maximal distance between two partons within a single jet, i.e. two partons form a jet only if their relative distance  $\Delta R_{ij}$  satisfies the condition

$$\Delta R_{ij} \leq \min \left[ \frac{E_{T_i} + E_{T_j}}{\max(E_{T_i}, E_{T_j})} R, R_{\text{sep}} \right]. \quad (12)$$

The question which value of  $R_{\text{sep}}$  to choose for the comparison of NLO parton level calculations with the results of the cone algorithm applied at the hadron level is nontrivial and we shall therefore present JETVIP results for both extreme choices  $R_{\text{sep}} = R$  and  $R_{\text{sep}} = 2R$ . To define momenta of jets JETVIP uses the standard  $E_T$ -weighting recombination procedure, which leads to massless jets. To assess the reliability of our conclusions we have furthermore investigated the following uncertainties:

**Choice of PDF:** We have taken CTEQ4M and SAS1D sets of PDF of the proton and photon respectively as our canonical choice. Both of these sets treat quarks, including  $c$  and  $b$  ones, as massless above their respective mass thresholds, as required by JETVIP, which uses LO and NLO matrix elements of massless partons. Taking into account our cuts on jet transverse energies, we set  $N_f = 4$  in any calculations discussed below. PDF of the proton are fairly well determined from global analyses of CTEQ and MRS groups and we have therefore estimated the residual uncertainty related to the choice of PDF of the proton by comparing the CTEQ4M results to those obtained with MRS(2R) set. The differences are very small, between 1.5% at  $\eta = 0$  and 3% at  $\eta = -2.5$ .

**Factorization scale dependence:** In principle proton and (in resolved channel) photon are associated with different factorization scales  $M_p$  and  $M_\gamma$ , but we followed the standard practice and set  $M_p = M_\gamma = M = \kappa(E_T^{(1)} + E_T^{(2)})/2$ . The factorization scale dependence was estimated by performing the calculations for  $\kappa = 1/2, 1, 2$ .

**Renormalization scale dependence:** The dependence of perturbative calculations on the renormalization scale  $\mu$  is in principle a separate ambiguity, unrelated to that of factorization scale  $M$ , but we followed the common practice and set  $\mu = M$ .

**Jet algorithm ambiguities:** To see how much our conclusions depend on  $R_{\text{sep}}$  we performed our calculations for two extreme values:  $R_{\text{sep}} = R, 2R$ .

**Hadronization corrections:** For any comparison of parton level calculations with experimental data understanding these corrections is crucial, but the problem is particularly pressing for jets with moderate  $E_T$ , like those used in all analyses of virtual photon structure. Hadronization corrections are not simple to define, but adopting the definition used by experimentalists [7], we have found that they depended sensitively and in a correlated manner on transverse energies and pseudorapidities of jets. For  $E_T^c = 5$  GeV they start to rise steeply below  $\eta \doteq -2.5$  and we therefore required both jets to lie in the region  $-2.5 \leq \eta^{(i)} \leq 0$ , where hadronization corrections are flat in  $\eta$  and do not exceed 20%.

For virtual photons JETVIP can be run in two different modes:

**DIR<sub>uns</sub>:** only the NLO unsubtracted direct photon calculations are performed without introducing the concept of virtual photon structure.

**DIR+RES:** employs the concept of PDF of the virtual photon and gives jet cross-sections as sums DIR+RES of subtracted direct and resolved photon contributions.

We first discuss results for the first window  $1.4 \leq P^2 \leq 2.4$  GeV<sup>2</sup>. In Fig. 7  $d\sigma/d\eta$  and  $d\sigma/dE_T$  distributions of trigger jets obtained within the DIR+RES approach are compared to those of DIR<sub>uns</sub> one. All curves correspond to  $R_{\text{sep}} = 2$ . The difference between the results of these two approaches is significant in the whole range of  $\eta$ , but particularly large close to the upper edge  $\eta = 0$ , where the DIR+RES results exceed the DIR<sub>uns</sub> ones by a factor of more than 3! In  $d\sigma/dE_T$  distributions this difference comes predominantly from the region of  $E_T$  close to the lower cut-off  $E_T^c + \Delta = 7$  GeV. Fig. 7 also shows that the scale dependence is nonnegligible in both approaches, but does not invalidate the main conclusion drawn from this comparison. The dependence of the above results on  $R_{\text{sep}}$  (not shown) is almost imperceptible for DIR<sub>uns</sub> calculations and below 10% for the DIR+RES ones. To track down the origins of the observed

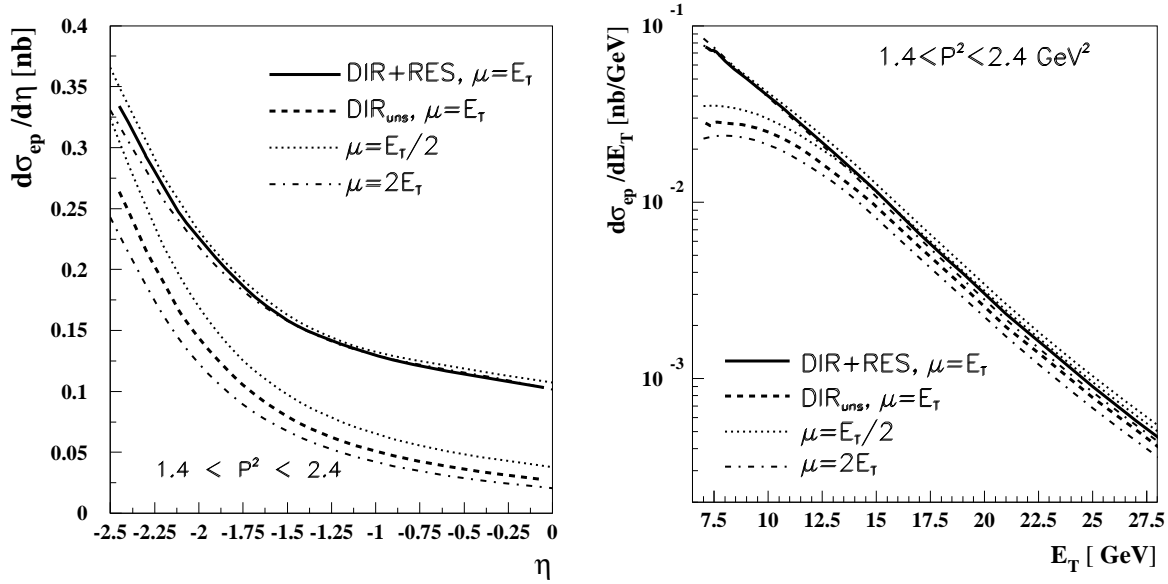


Figure 7: Scale dependence of the distributions  $d\sigma/d\eta$  and  $d\sigma/dE_T$  at the NLO. All curves correspond to  $R_{sep} = 2R$ . The dotted and dashed-dotted curves have the same meaning for DIR+RES as well as DIR<sub>uns</sub> calculations.

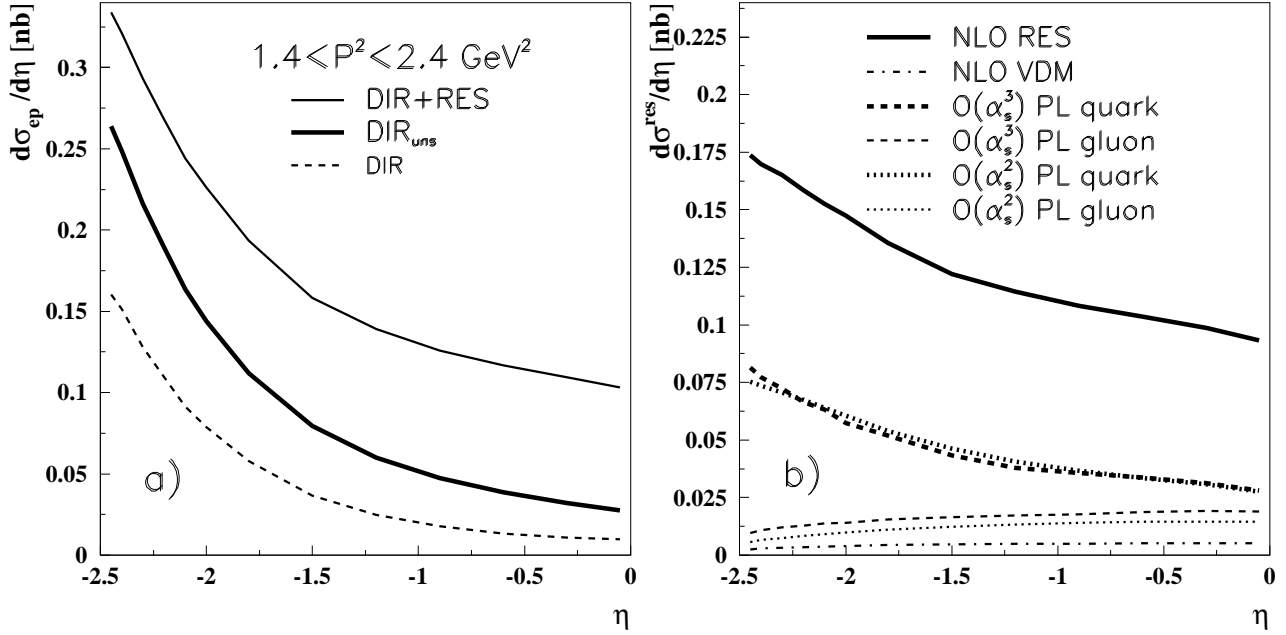


Figure 8: Comparison of DIR+RES, DIR<sub>uns</sub> and DIR results for  $d\sigma/d\eta$  (a). In b) individual contributions to  $d\sigma_{NLO}^{res}/d\eta$  are plotted.

large differences between DIR+RES and DIR<sub>uns</sub> results, we did two simple exercises. In Fig. 8a the DIR+RES and DIR<sub>uns</sub> results are compared to the subtracted direct (DIR) ones. The difference between the DIR+RES and DIR curves, defining the resolved photon contribution  $d\sigma^{\text{res}}/d\eta$ , is then split into the contributions of:

- the VDM part of photonic PDF convoluted with complete NLO (i.e. up to the order  $O(\alpha_s^3)$ ) parton level cross-sections (denoted NLO VDM),
- the pointlike quark and gluon distribution functions convoluted with  $O(\alpha_s^2)$  and  $O(\alpha_s^3)$  parton level cross-sections

and plotted in Fig. 8b. Fractional contributions of LO (i.e.  $O(\alpha_s^2)$ ) and NLO (i.e.  $O(\alpha_s^2) + O(\alpha_s^3)$ ) terms to  $\sigma^{\text{res}}$  are plotted in Fig. 9a as functions of  $\eta$ . Several conclusions can be drawn from Figs. 8–9:

- The contribution of the VDM part of photonic PDF is very small and perceptible only close to  $\eta = 0$ . Integrally it amounts to about 3%. Using SaS2D parametrizations would roughly double this number.
- The inclusion of  $O(\alpha_s^3)$  resolved photon contributions is numerically important in the whole range  $-2.5 \leq \eta \leq 0$ . Interestingly, throughout this interval the  $O(\alpha_s^3)$  results, particularly those of pointlike quarks, are close to the  $O(\alpha_s^2)$  ones.
- At both  $O(\alpha_s^2)$  and  $O(\alpha_s^3)$  orders pointlike quarks dominate  $d\sigma^{\text{res}}/d\eta$  at large negative  $\eta$ , whereas as  $\eta \rightarrow 0$  the fraction of  $d\sigma^{\text{res}}/d\eta$  coming from pointlike gluons increases towards about 40% at  $\eta = 0$ .

We reiterate that pointlike gluons carry nontrivial information already in convolutions with  $O(\alpha_s^2)$  partonic cross-sections because in unsubtracted direct calculations such contributions appear first at the so far uncalculated order  $\alpha\alpha_s^3$ . The results of pointlike quarks convoluted with  $O(\alpha_s^3)$  partonic cross-sections would be included in unsubtracted direct calculations starting at the order  $\alpha\alpha_s^3$ , whereas for pointlike gluons this would require evaluation of unsubtracted direct terms of even higher order  $\alpha\alpha_s^4$ ! In JETVIP the nontrivial aspects of taking into account the resolved photon contributions can be characterized<sup>5</sup> by the “nontriviality fractions”  $R_3, R_4$

$$R_3 \equiv \frac{q^{\text{PL}} \otimes \sigma_q^{\text{res}}(O(\alpha_s^3)) + G^{\text{PL}} \otimes \sigma_G^{\text{res}}(O(\alpha_s^2))}{\sigma^{\text{res}}}, \quad R_4 \equiv \frac{G^{\text{PL}} \otimes \sigma_G^{\text{res}}(O(\alpha_s^3))}{\sigma^{\text{res}}}, \quad (13)$$

plotted as functions of  $\eta$  and  $P^2$  in Fig. 10. Note that at  $\eta = 0$  almost 70% of  $\sigma^{\text{res}}$  comes from these origins. This fraction rises even further in the region  $\eta > 0$ .

So far we have discussed the situation in the first window  $1.4 \leq P^2 \leq 2.4 \text{ GeV}^2$ . As  $P^2$  increases the patterns of scale and  $R_{\text{sep}}$  dependences change very little. On the other hand, the fractions plotted in Fig. 9 and 10 vary noticeably:

- The unsubtracted direct photon contributions (DIR<sub>uns</sub>) represent increasing fractions of the full NLO JETVIP results.

---

<sup>5</sup>Disregarding the VDM part of resolved contribution which is tiny in our region of photon virtualities.

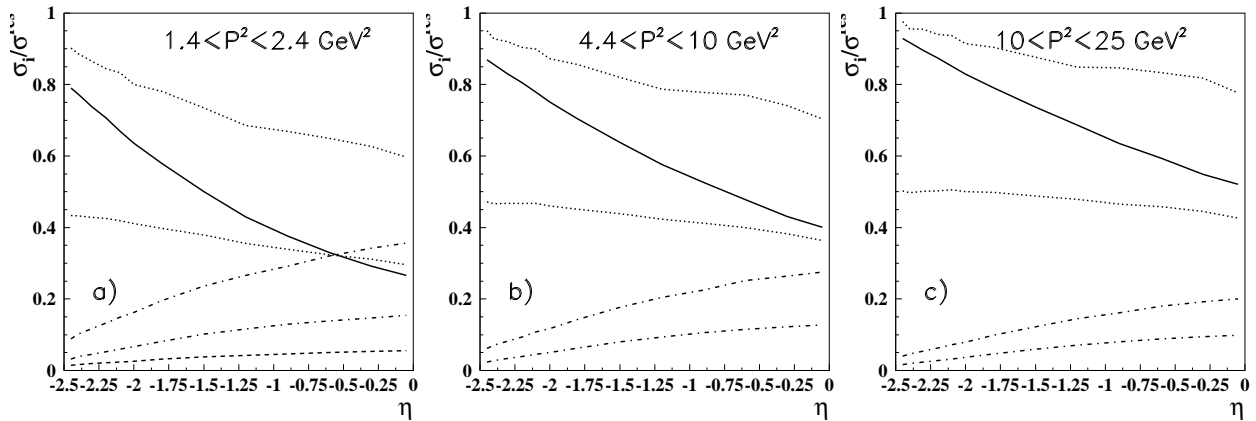


Figure 9: *Fractional contributions to  $\sigma^{\text{res}}$ . Upper and lower dotted (dashed-dotted) curves correspond to pointlike quarks (gluons) convoluted with NLO and LO partonic cross-sections. The lower dashed curve in a) gives the NLO VDM contribution. The solid curves show the ratio of NLO DIR<sub>uns</sub> calculations to the NLO DIR+RES ones.*

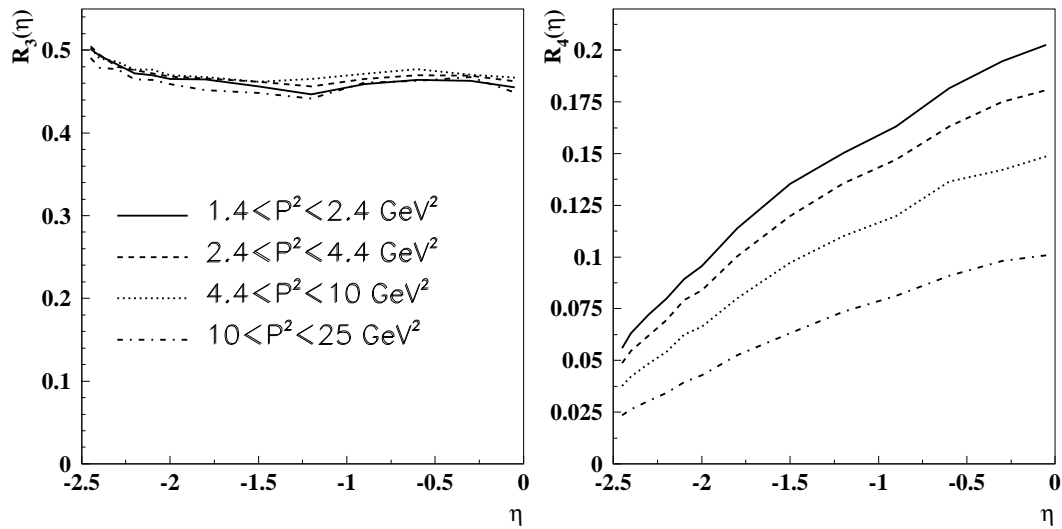


Figure 10: *Nontriviality fractions  $R_3$  and  $R_4$  as functions of  $\eta$  and  $P^2$ .*

- The relative contribution of pointlike gluons with respect to pointlike quarks decreases.
- The nontriviality factor  $R_4$  (which comes entirely from pointlike gluons) decreases, whereas  $R_3$ , which is dominated by pointlike quarks and flat in  $\eta$ , is almost independent of  $P^2$ .

All these features of JETVIP calculations reflect the fundamental fact that as  $P^2$  rises towards the factorizations scale  $M^2 \approx E_T^2$  the higher order effects incorporated in pointlike parts of photonic PDF vanish and consequently the unsubtracted direct results approach the DIR+RES ones. The crucial point is that for pointlike quarks and gluons this approach is governed by the ratio of  $P^2/M^2$ . The nontrivial effects included in PDF of the virtual photon thus persist for arbitrarily large  $P^2$ , provided we stay in the region where  $P^2 \ll M^2$ .

## 5 Summary and conclusions

We have analyzed the content of parton distribution functions of the virtual photon within the framework of SaS approach to their parametrization. In this approach, quark as well as the gluon distribution functions can be separated into the nonperturbative VDM and pointlike parts, the latter being in principle calculable by perturbative means. The inherent ambiguity of this separation, numerically large for the real photon, becomes phenomenologically irrelevant for virtual photons with  $P^2 \gtrsim 3 \text{ GeV}^2$ . In this region quark and gluon distribution functions of the virtual photon are dominated by their (reasonably unique) pointlike parts, which have clear physical origins. We have analyzed the nontrivial aspects of these pointlike distribution functions and, in particular, pointed out the role of pointlike gluons in leading order calculations of jet cross-section at HERA.

At the NLO we have found a significant difference between JETVIP results in approaches with and without the concept of virtual photon structure. While for the real photon analogous difference is in part ascribed to the VDM components of photonic PDF, for moderately virtual photons it comes mostly from pointlike quarks and pointlike gluons. Although their contributions are in principle contained in higher order direct photon calculations, to get them in practice would require calculating at least  $O(\alpha\alpha_s^3)$  and  $O(\alpha\alpha_s^4)$  unsubtracted direct contributions. In the absence of such calculations the concept of PDF of the virtual photon is therefore phenomenologically indispensable.

We have also shown that despite the expected dominance of the transversely polarized photons, the longitudinal polarization of virtual photons may play a numerically important role in the region of moderate virtualities accessible at HERA and should therefore be taken into account in analyses of relevant experimental data.

**Acknowledgments:** We are grateful to G. Kramer and B. Pötter for discussions on the interactions of virtual photons and to B. Pötter for help with running JETVIP.

## References

- [1] G. Schuler, T. Sjöstrand, *Z. Phys. C* **68**, 607 (1995)
- [2] G. Schuler, T. Sjöstrand, *Phys. Lett. B* **376**, 193 (1996)
- [3] J. Chýla, hep-ph/9811455
- [4] C. Adloff et al (H1 Collab.), DESY 98-205, hep-ex/9812024
- [5] B. Pötter, *Comp. Phys. Comm.* **119**, 45 (1999)  
G. Kramer, B. Pötter, *Eur. Phys. J.* **C5**, 665 (1998)
- [6] S. Frixione, G. Ridolfi, *Nucl. Phys. B* **507**, 295 (1997)
- [7] C. Adloff et al (H1 Collab.), *Eur. Phys. J.* **C5**, 625 (1998)